FLOW OBSERVATIONS AT A VERTICAL DROP STRUCTURE

RAFAEL MURILLO-MUÑOZ
School of Civil Engineering, University of Costa Rica, Costa Rica, E-mail: rmurillo@eic.ucr.ac.cr

ABSTRACT

Results from an experimental study conducted to investigate the characteristics of the velocity field along the jet trajectory of a drop structure are presented. Constant temperature anemometry is used for detailed quantitative measurements of the air-water flow characteristics. The measurements indicate the occurrence of four different velocity profiles along the jet path. At the brink, a non-uniform velocity profile is observed while at the free falling jet a uniform one. On the sliding jet, the profiles resemble those of a submerged turbulent jets and at the drop base, the shape of the profile is fairly uniform. Moreover, in the cases of a fully aerated and non-aerated drop structure, it is found that there is no significant difference in the velocity profile of the sliding jet. In addition, measurements of local void fraction indicate the presence of air bubbles inside the recirculating pool area only. These bubbles are likely brought into this area by a mechanism similar to that of a plunging jet.

KEY WORDS: drop structures; velocity; jets

INTRODUCTION

The drop structure has received significant attention for over 70 years. The flow over this structure is divided into the free falling jet, the sliding jet and the recirculating pool in the case of a fully ventilated nappe (Figure 1a). If ventilation is not provided to the lower nappe, only the sliding jet and the recirculating pool would form (Figure 1b). Some early works about the drop structure include Rouse (1936), Moore (1943), Rand (1955), Rajaratnam and Muralidhar (1968), Gill (1979), Hager (1983), Chamani (1993), Rajaratnam and Chamani (1995) as well as Lin et al. (2002) among many others.

Chamani (1993), Rajaratnam and Chamani (1995) as well as Lin et al. (2002) provided velocity measurements in the sliding jet. Chamani (1993), using a Prandtl tube concluded that the velocity distribution in the sliding jet is not uniform and decreases continuously towards the pool. Based on these observations, these authors considered the shear force between the sliding jet and the pool to be the main factor in energy dissipation. Rajaratnam and Chamani (1995) support these observations and further noted that the velocity profiles in the sliding jet resembled those in submerged turbulent jets.

On the other hand, Lin et al. (2002) performed a study of the velocity field in the sliding jet and the recirculating pool. Using fiber laser doppler velocimetry they concluded that the velocity distribution across the jet is uniform until the jet touches the boundary of the pool. They also indicated that the profiles are similar to those in turbulent jets. Using visualization techniques, they

also observed the shear layer between the sliding jet and the pool, where they observed there is strong mixing and the velocity field varies sharply.

In this contribution the velocity profiles along the jet trajectory are analyzed in order to clearly observe the changes that the profiles undergo along the path of the jet, from the brink to the drop base. A quantification of the local void fraction along the trajectory is also attempted.

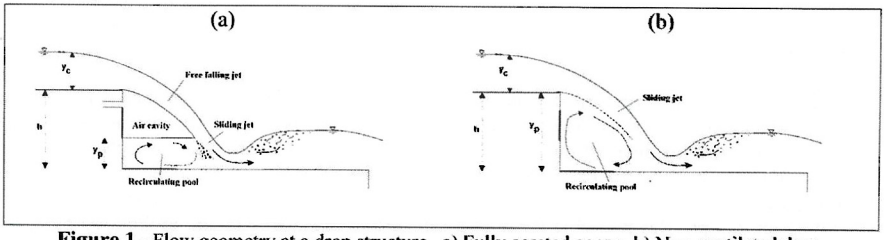

Figure 1.- Flow geometry at a drop structure. a) Fully aerated nappe. b) Non-ventilated drop.

EXPERIMENTAL SETUP

The flow over a drop structure was examined as part of a larger study dealing with the development flow region on stepped chutes (Murillo-Muñoz, 2006). The geometric similarity between a drop structure and the first step of a stepped chute allowed for this examination. The model of the stepped chute was made of HDO plywood and it had a rectangular cross section with a horizontal channel to provide a subcritical flow approach. Steps on the chute had a height (h) of 15 cm and a tread length (L) of 75 cm. Water was supplied to the model by a 60 cm PVC pipeline while the flow was controlled using a 1:50 butterfly valve. To quantify the flow, a MSR Magmeter® (Magnun Standard) was installed on the supply line and a LabVIEW® virtual instrument was developed in order to process the flow data in real time. The MSR Magmeter was calibrated in situ via an 7.5 m^3 volumetric tank.

The experimental observations were carried out using a conical hot-film probe (Dantec Dynamics, 55R42) in conjunction with a DISA 55M constant temperature anemometer equipped with a standard bridge (55M10). The anemometer was operated with a constant overheat ratio of 10%. Initial testing indicated that this ratio value provided adequate signal sensitivity while keeping a low risk of bubble formation. Water temperature was collected using a digital platinum resistance thermometer (Guildline, 9540) with a resolution of 0.01 °C. The observed water temperature drift was less than 0.1 °C and thus, adjustments to the overheat ratio were unnecessary. No filtration or heating/cooling units were employed and tap water from the city main was used in the laboratory recirculating system. Calibration of the conical probe was performed using a water tunnel connected to laboratory recirculating system. Figure 2 shows the probe calibration at two different temperatures. In this figure U is the flow velocity and E is the anemometer output voltage. To detect probe contamination, calibrations were performed before and after each experiment. However, probe contamination was not an issue during the tests.

Anemometer output voltages were collected using a National Instrument® data acquisition card (PCI-MIO-16E-4) and uploaded to a personal computer using LabVIEW®. Data acquisition was performed at 5000 Hz for a 180 second duration with a precision of ±1.22 mV. Analysis of the anemometer signal was carried out using MatLab® and following the methodology described by Farrar et al. (1995) to separate the two phases of the flow.

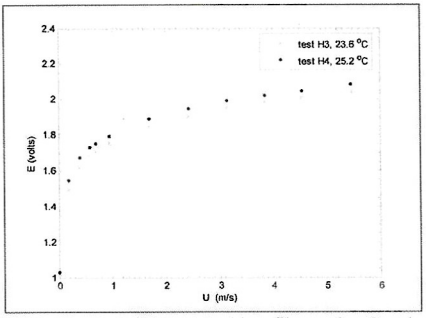

Figure 2.- Calibration curves of the conical hot-film probe. Overheat ratio of 10%.

EXPERIMENTAL RESULTS

Several profiles were taken on the width centerline along the jet trajectory using the conical hot-film probe. Figure 3 indicates the locations of the profiles for the case of a fully ventilated drop structure. The approach flow to the brink was always subcritical and velocity profiles for two discharges at this location are given in Figure 4a. The profiles at this section are not uniform and they present larger velocities closer to the bottom. Rajaratnam and Muralidhar (1968) as well as Chamani (1993) measured similar profiles. Detailed measurements of the instantaneous characteristics of the velocity field are given by Murillo-Muñoz (2006).

Figure 4b gives the velocity distribution in the midsection of the free falling jet. In this figure, the parameter y_{jet} corresponds to the actual thickness of the jet. This profile was taken at a tilt angle of 41° and it is quite distinctive from the one at the brink. The velocity field has redistribute and resembles a plug flow, although it has a small "S" shape were the velocities on the top half of it have increased considerable with respect to those values at the brink, possible due to gravitational effects. At the lower nappe they have increased slightly in accordance with the new boundary conditions, i.e., air. The measured profile agrees in general terms with the ones given by Chamani (1993) but unfortunately, the level of detail presented by Chamani was not enough to allow an adequate comparison.

Velocity profiles in the midsection of the sliding jet are given in Figure 4c. These profiles were taken at tilt angles of 45° $\left(y_c/h = 0.489\right)$ and 40° $\left(y_c/h = 0.779\right)$. Rajaratnam and Chamani (1995) as well as Lin et al. (2002) observed that the velocity profile of the sliding jet resembles those of submerged turbulent jets. Thus, the ordinates of this figure were normalized using the water depth b, which corresponds to the water depth at a flow velocity of $0.5U_{\max}$. These measured profiles in the sliding jet showed the interaction effects of the recirculating pool. Lower velocities were measured on the bottom section of the jet while larger ones were measured at the top, resembling a uniform velocity profile. This re-arrangement of the profile is likely to be caused by the strong interaction between the recirculating pool and the jet. Moreover, this interaction developed velocities in the recirculating pool and therefore there is a profile inside the pool, in which the decrease in velocity is less abrupt.

Finally, the velocity field at the base of the drop structure is giving in Figure 4d. The shape of this profile is fairly uniform and they are in agreement with those reported by Bakhmeteff and Feodoroff (1943). Downstream of this location the observed flow was always supercritical.

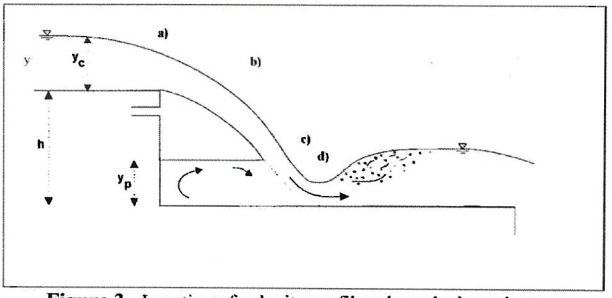

Figure 3.- Location of velocity profiles along the jet trajectory of a fully aerated drop structure.

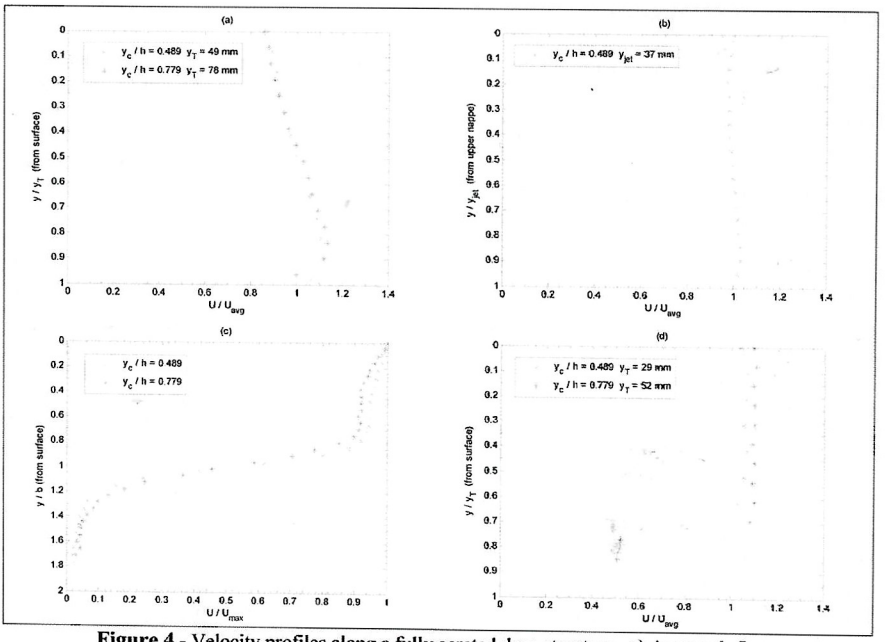

Figure 4.- Velocity profiles along a fully aerated drop structure. a) Approach flow. b) Free falling jet. c) Sliding jet. d) Drop structure base.

Similar to velocity, the local void fraction was measured at the brink, the free falling jet, the sliding jet and the base of the drop structure. Negligible values were measured in all sections but at the sliding jet. Figure 5 presents the measured local void fraction profiles. At the sliding jet, values of local void fraction were measured inside the recirculating pool and not at the jet core. This indicates that air bubbles are taken from the air cavity by the free falling jet which brings them into the pool. The mechanism to entrain this air would be similar to that of a plunging jet.

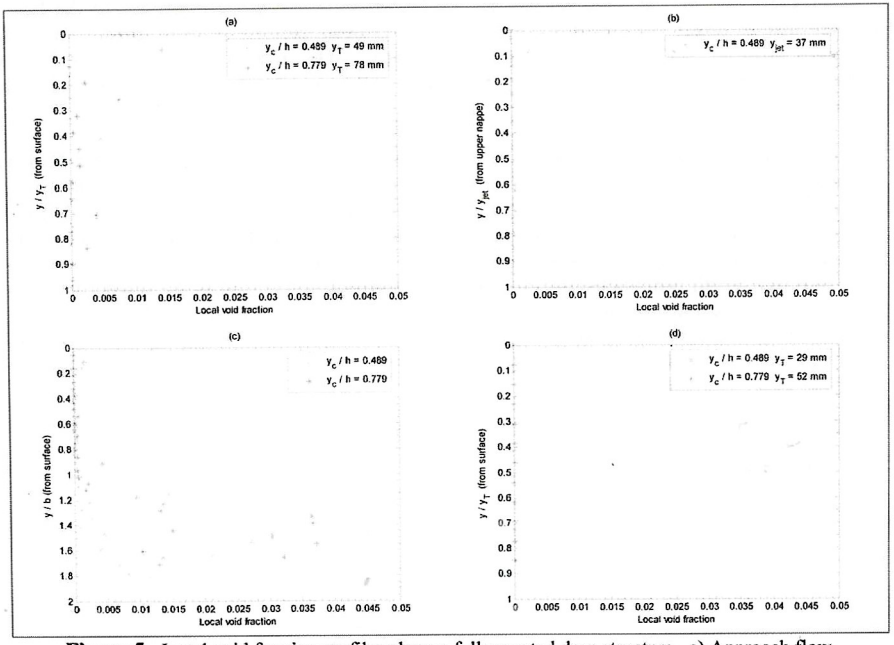

Figure 5.- Local void fraction profiles along a fully aerated drop structure. a) Approach flow. b) Free falling jet. c) Sliding jet. d) Drop structure base.

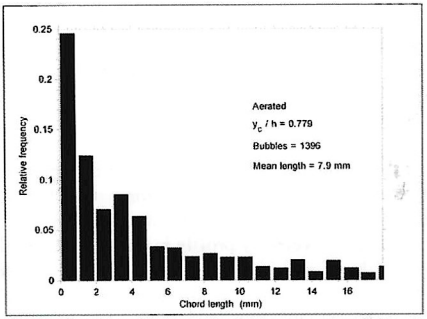

Figure 6.- Chord length distribution on the sliding jet for a fully aerated drop structure.

The chord length distribution at the midsection of the sliding jet is presented in Figure 6. This figure corresponds to a fully aerated drop structure. As mentioned before, local void fraction was only detected inside the recirculating pool. Thus, the distribution shown in Figure 6 corresponds to the values of local void fraction indicated in Figure 5c.

Finally, the cases of a fully aerated drop structure and a non-aerated are given in Figure 7. Velocity profiles shown on this figure correspond to the midsection of the sliding jet. Broadly

speaking, the figure indicates that all profiles are fairly similar. A close inspection of the figure indicates that at larger discharges the similarity on velocity profiles is quite good. At small discharges however, the profiles have small differences. The aerated condition has a slightly sharper transition from the jet area to the pool area as well as an almost vertical distribution inside the recirculating pool.

Moreover, in the case of a fully aerated drop structure, the observations of the velocity profiles also suggest an influence of the recirculating pool on the sliding jet. At small discharges the length of the sliding jet is smaller (larger air cavity) and therefore there is less possibility of energy dissipation at the interface between the jet and the pool. Hence, at small discharges the profiles would differ since there is a slim possibility of interaction while at large discharges the larger interface length benefits the interaction. The difference is reflected as the sharper transition and an almost vertical distribution mentioned before. In the case of a fully depleted jet (non-aerated case), the length is maximized and consequently, the velocity profiles would agree as observed. Finally, measurements of local void fraction on the case of a non-ventilated drop structure indicated negligible values along the jet trajectory.

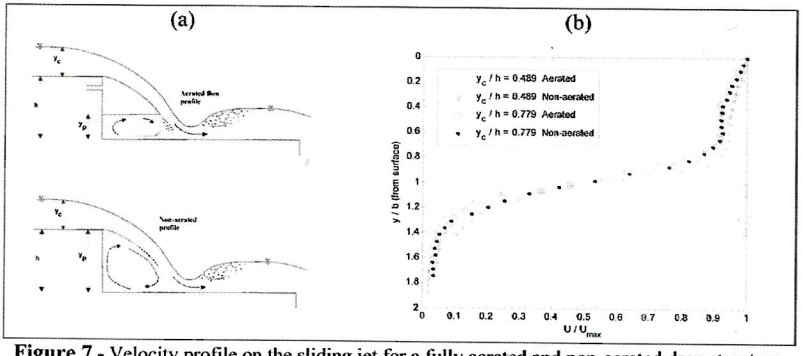

Figure 7.- Velocity profile on the sliding jet for a fully aerated and non-aerated drop structure. a) Profile locations. b) Velocity profiles.

CONCLUSIONS

Taking advantage of the geometric similarity between a drop structure and the first step of a stepped chute, several measurements were carried out on a model of the latter structure. It was found that the velocity field of a fully aerated drop structure suffers several modifications along the trajectory of the jet. At the brink, the velocity profile is not uniform while at the free falling jet the distribution resembles the profile of a plug flow. At the sliding jet, the distribution is modified again and at this location the profile is similar to the distribution of a submerged turbulent jet. At the base of the drop structure the velocity profile changes once more and it takes a fairly uniform shape. In the case of non-aerated drop structure, the sequence of profiles is as follows: non-uniform at the brink, submerged turbulent jet profile at the sliding jet and a uniform profile at the drop base.

Measured values of local void fraction were negligible in all sections with the exception of the sliding jet. At this location however, measurements indicated the presence of air bubbles inside the recirculating pool only, and not at the jet core. It is theorized that these bubbles are brought from the air cavity into the recirculating pool by a mechanism similar to the one in a plunging jet. Finally, the experimental results indicated that there is no significant difference in velocity profile between the sliding jet of an aerated drop structure and the sliding jet of a non-aerated.

Measurements also indicated insignificant values of local void fraction in the case of a non-aerated drop structure.

ACKNOWLEDGMENT

Support for this study was provided by the Natural Science and Engineering Research Council (NSERC), Canada, and Manitoba Hydro's Research and Development Program (Project G168). This research was carried out at the Hydraulics Research & Testing Facility, Department of Civil Engineering, University of Manitoba, Canada.

NOTATION

b: water depth at $0.5U_{max}$;
E: anemometer output voltage;
h: step height;
U: water flow velocity;
U_{avg}: mean water flow velocity;
U_{max}: maximum water flow velocity;
y: water depth;
y_c: critical water depth;
y_{jet}: thickness of the free falling jet;
y_p: pool water depth;
y_T: total water depth;

REFERENCES

Bakhmeteff, B.A. and Feodoroff, N.V. (1943). "Discussion of Moore (1943)". *Transactions*, ASCE, Vol. 108, pp. 1364-1373.

Chamani, M.R. (1993). "Jet flow on stepped spillways and drops". M.Sc. thesis, University of Alberta. Alberta, Canada.

Farrar, B.; Samways, A.L.; Ali, J. and Bruun, H.H. (1995). "A computer-based hot-film technique for two-phase flow measurements". *Measurement Science and Technology*, Vol. 6, No. 10, pp. 1528-1537.

Gill, M.A. (1979). "Hydraulics of rectangular vertical drop structures". *Journal of Hydrulic Research*, IAHR, Vol. 17, No. 4, pp. 289-302.

Hager, W. (1983). "Hydraulics of plane free overfall". *Journal of Hydraulic Engineering.*, ASCE, Vol. 109, No. 12, pp. 1683-1697.

Lin, C.; Huang, W.Y.; Suen, H.F.; Hsieh, S.C. (2002). "Study on the characteristics of velocity field of free overfalls over a vertical drop". *Hydraulic Measurements and Experimental Methods 2002*, ASCE, U.S.A., pp. 178-187.

Murillo-Muñoz, R.E. (2006). "Experimental study of the development flow region on stepped chutes". Ph.D. thesis, University of Manitoba. Manitoba, Canada.

Moore, W.L. (1943). "Energy loss at the base of a free overfall". *Transactions*, ASCE, Vol. 108, pp. 1342-1360.

Rajaratnam, N. and Chamani, M.R. (1995). "Energy loss at drops". *Journal of Hydraulic Research*, IAHR, Vol. 33, No. 3, pp. 373-384.

Rajaratnam, N. and Muralidhar, D. (1968). "Characteristics of the rectangular free overfall". *Journal of Hydraulic Research*, IAHR, Vol. 6, No. 3, pp. 233-258.

Rand, W. (1955). "Flow geometry at straight drop spillways". *Proceedings*, ASCE, Vol. 81, September, paper 791.

Rouse, H. (1936). "Discharge characteristics of the free overfall". *Civil Engineering*, ASCE, Vol. 6, No. 4, pp. 257-260.